DWT based Image Super Resolution using Segmentation and Edge Detection

*Prathibha Kiran[1], and Fathima Jabeen[2]

[1]Research Scholar, Bengaluru, VTU, India.
prathibha.swamy87@gmail.com

[2]Islamiah Institute of Technology, Bengaluru, VTU, India
rawoof500@gmail.com

Abstract

An image super-resolution is the development of creating a high-resolution image from low-resolution images for better image visualization for several recent applications. In this research paper, we propose DWT-based Image Super Resolution using Segmentation and Edge Detection for better picturing of images. The different kinds of colore images are considered and converted into greyscale images and resized to a uniform size of 166x304. The Discrete Wavelet Transform (DWT) is used to get one low-frequency and three high-frequency bands with a size of 83x152. The four bands are fused and dividing each coefficient by two to get Low Resolution (LR) images. Each coefficient of the LR image is inflated into 2x2 coefficients to get High Resolution (HR) image. The HR matrix is segmented into a 3x3 overlapped matrix and an average value is calculated and assigned to the whole HR matrix. The Canny edge detection is used on the original image to get the edge detected image. The pixel values of HR and canny edge detected images are compared and high-value coefficients are considered. The guided filter is applied to the high-value coefficients matrix to improve the quality of the image by refining the image. The LL band of the DWT matrix is padded with zeros to convert matrix size to 166x304 and Inverse Discrete Wavelet Transform (IDWT) is used on it. The refined and IDWT images are merged by computing the average values to acquire Super Resolution (SR) image. It is noted that the anticipated system results are enhanced compared to current methods.

Keywords: *DWT, Fusion, Image Processing, Segmentation, Super Resolution*

1. Introduction

In recent years there is a tremendous demand for HR images for correct investigation in diverse fields of applications. Digital picture processing is encouraged through the reality that almost all of the facts acquired through a person are visible, it turned into felt that a success integration of the capacity to procedure visible facts right into a device might make contributions to improving its usual facts processing power. Resolution is possibly a complicated time period in describing the traits of a visible picture because it has a massive quantity of competing phrases and definitions. In its most effective form, picture decision is described because the smallest discernible or measurable element in a visible presentation. These days, picture processing strategies are implemented to a extensive sort of regions inclusive of robotics, business inspection, far flung sensing, picture transmission, clinical imaging, surveillance, etc. In nearly every application, it's far perfect to generate a picture that has a totally excessive decision. Thus, a totally excessive-decision picture ought to make contributions to a higher class of areas in a multi-spectral picture or to extra correct localization of a place of hobby in a picture or ought to facilitate a extra eye-catching view in excessive-definition televisions (HDTV) or web-primarily based totally pics. In maximum digital imaging applications, pics with HR are favored and frequently required. In the HR pics, the pixel density is excessive and consequently can provide extra info that can be required in diverse applications. For instance, HR clinical pics are beneficial for medical doctors and a good way to make the appropriate diagnosis.

The SR is a class of methods that improve the resolution of an image from one or more LR images that have been produced from a particular imaging system. The Image SR algorithms undertaken three significant stages viz., the

Interpolation, the SR Reconstruction and Learning based SR methods. Nearest Neighbor Interpolation is the modest practice in Interpolation which determines the nearest neighboring pixel and each interpolated output pixel is allocated the value of adjacent sample point in input image. It is simplest and fastest implementation of image scaling method which is very valuable when rapidity is of the chief worry. One of the examples is to zoom an image for editing purpose. It does not change the actual values but it is ideal if suitable variations in the grey level values want to be retained. One of the major advantages is, it requires least processing time because it takes only one pixel into consideration i.e. nearest one to interpolated point. The effect of this is making each pixel larger in size which results in heavy jagged edges and the visual distortion occur which is again an aspect of poor image.

Nowadays, deep learning has become more popular which uses Convolution Neural Network (CNN) for super resolution. Sparse coding based SR technique is redeveloped into a deep CNN for SR. An end-to-end plotting between LR and HR images is learnt directly. The deep CNN converts LR images into HR images by mapping. In this method, at first Bi-cubic Interpolation upscale a single LR image. This interpolated technique extracts areas with high dimensional vector and is mapped onto another high dimensional vector that represents HR patch. The reconstruction is used to collective the high-resolution patches to generate HR image. SR - CNN robustness is used for image de-blurring and de-noising low-level vision problems. The reconstructed image of the network of CNN-SR generally suffers from some ringing and jaggy artifacts. Thus, novel priori, an SR technique is established with the limitation of gradient fields which can eliminate artifacts from recreated HR images but cannot reinstate details and fine assemblies. The HR images are evaluated with extra fine structures but fewer artifacts, a Single Image Super-Resolution (SISR) based on Deep Learning and Gradient Transform. CNN for the gradient is trained to transform the gradients of an up-scaled image into desired gradients that are purer and sharper.

Contribution*:* The SR procedure is used in image processing applications to enhance perceptibility for a healthier empathetic of images. The contributions of the research are as follows

(i)   The LR images are transformed into intermediate High Resolution (HR) images by expanding each pixel to 4 pixels in the form of 2X2 blocks

(ii)The HR images are segmented into 3X3 overlapping blocks to find the average values of 9 pixels in each block to make the smooth image with the nearest pixel. The image size is decreased to 164X302 hence to get the image size equal to the reference image, repeat the boundary coefficient to obtain 166X304

(iii) The edge detection using a canny filter is used to detect the edge of the original image

(ii) The guided filtering for edge-preserving smoothing on an image and edge sharpening is applied to an average pixel image.

(iii) The sharper image is fused with IDWT image by finding the average to obtain the SR Image.

This research is prearranged as follows; section 2 brings the literature survey of SR. Section 3 offers the circumstantial of DWT, canny edge detection, and guided filter. The projected system details are given in Section 4. The anticipated algorithm is specified in section 5. Section 6 discusses the outcomes of the research. The conclusion and future work are stated in Section 7.

2. Literature Survey

The review of the SR using spatial and transform domains is pronounced in this section to realize and discover the research limitations.

Wenbin Li et al., [1] planned a scheme that involves image decomposition, morphological component examination, and coupled dictionary learning where LR images and texture are used to develop dictionaries. This method improved the mapping relationship between the LR image and HR texture layers that enhanced quality. The model produced healthier outcomes in the peak signal-to-noise ratio and structural similarity. Deeba et al., [2] anticipated the super-resolution based on a wavelet deep neural network model for a single image. The SWT is used for upscaling property. Trinh et al., [3] planned a technique for SR of medical images with de-noising. This scheme exploits standard images for the building of the database of HR and LR patch pairs. In the database with a Sparse positive linear representation of the HR patches, the problem is framed as a sparse decomposition optimization badly behaved with a penalty function stated in terms of the difference among patches to enforce sparsely and the excellence of the SR result. In

[4], anticipated a SR method with DWT to get high-frequency subbands and are interpolated to obtain the high-resolution image. The SWT is utilized to increase the edges. Gungor Polatkan et al., [5] developed Image SR based on the Bayesian non-parameter method. The process used Gibbs sampling and the Online Variation Bayes algorithm. The results were verified on both benchmarks and natural images with several models from the literature. In order to access the visual excellence of the outcomes the first execution method used was Gibbs Sampling which later was found to be non-feasible for large-scale data.

Dai-Viet Tran et al., [6] presented an approach known as Example-Based SR for improving the spatial resolution of medical images embedded with noise. In this method with aid of previously current databases constructed, HR image is reconstructed from LR image based on sparsity of patches. The concept of EMD (Earth Movers Distance) was introduced to measure the similarity among the image patches which only selects the most likely candidates are used in the optimization problem. Results show that the proposed algorithm offers a better efficiency with the noise corrupted with LR image when compared with the other existing SR methods. In order to select image patch L norm threshold of EMD-based distance was established. But it is highly time-consuming and it is metric only for normalized distributions. Jingxu Chen et al., [7] developed a deep learning technique and gradient conversion method for SR method. The CNN in gradient field is trained to alter the gradients of the up-scaled image into the wanted gradients using Gradient Transformation network. To create the reconstruction energy function the converted gradients are exploited as a restriction. Results shows that the recreated HR images of the proposed process achieve high refurbishment excellence and produces sharp HR images with few artifacts. Therefore Super Resolution methods with the restriction of gradient fields are developed. CNN is utilized for gradient transformation. Mean Squared Error (MSE) is used as the loss function to train network and Back propagation algorithm is used to lessen the loss function. The HR image is predictable by improving the energy function.

 Haijun Wang et al., [8] proposed a influential and sophisticated probabilistic learning tool known as GPR (Gaussian Process Regression) for learning the non-linear mapping from an experiential space to an predictable latent space. The GPR is used on learning based SR, the time complexity of GP is high for bulky datasets and for the SR reconstruction the Gaussian likelihood in GPR is not suitable. Aiming at these issues a GPR based SR method by integrating dictionary based sampling (Dbs) strategy and GPR prototypical with Student-likelihood. To reduce the computational complexity Dbs strategy by joining all the neighbourhood samples of every atom into a compact illustrative training subset was developed. Junjun Jiang et al.,[9] planned a image SR method via locally Regularized Anchored Neighbourhood Regression and Non-Local Means which generates visually pleasing HR image from a given LR input. Locally constraint is used to choice dictionary atoms and allocates dissimilar freedom to each dictionary atom affording to its association to the input LR patch. Thus by presenting this flexible priori, the planned technique reports the problem of learning the mapping functions among LR and HR images based on each dictionary of LR and HR examples and generates the results with rich textures. ANR (Anchored Neighbourhood Regression) based SR method is used as a initial point for SISR method by Regression based SR with Non-Local Means (LANR-NLM). Oliver Bowen and Christos-Savvas Bouganis [10] presented a real-time SR using an FPGA device. In this approach a bunch of overlapping LR images are combined to generate a single HR image. A weighted mean SR algorithm has been joint with the current fast and robust multi-frame SR algorithm to improve the quality of the image.

Weiguo Yang et al., [11] introduced a dictionary learning and morphological component analysis (MCA)-based image super resolution technique. An image is divided into texture and structure components using the MCA. The texture component trains the dictionary. The structural part uses bicubic interpolation, while the texture part is rebuilt using sparse depiction.Cao et al., [12] proposed a face image rebuilding technique based on wavelet transform and SR generative adversarial network (SRGAN). The LR face image is preprocessed by wavelet transform algorithm to get the thorough texture features of the face image under dissimilar frequencies. The GAN is used to learn the prior knowledge of wavelet transform coefficients. The identity preserving constraint is used on the images. The deep learning model based on SRGAN is used to acquire HR face images. Shivagunde and Biswas [13] planned better interpolation technique for obtaining of HR image. The LR patch interpolated and equivalent HR patch pixel values using multilayer perceptron (MLP) and DWT for producing eccentric HR. A review research paper [14] was published to identify the different image SR algorithms to enhance LR images to HR images. The author provided a detailed explanation of the various SR approaches and their applications.Zhang et al., [15] Single-Image SR based on

Rational Fractal Interpolation was projected. By combining rational and fractal interpolation, formed a bivariate rational fractal interpolation model and investigated its analytical assets. Nakahara et al., [16] projected a learning-based technique with a small number of filters for single image SR. For hash calculation, the technique necessitates a change in geo-metric flip and revolution addition. The image SR using DWT [17] with zooming Learning features from HR images improves the LR image. The method employed four neighbourhoods pixels estimation and DWT to extract detailed info from the training database and to investigate high frequency coefficients of HR exercise images. C Lien et al., [18] planned a learning-based SR technique with wavelet coefficients estimation to reconstruct the HR images. Dhara and Sen [19] offered an interpolated SR method that performs approximations of high frequency components by manipulating similarities in the process of wavelet breakdown of an image. The intended attenuation is achieved by the proper combination of DWT and stationary wavelet transform (SWT).

3. Background

3.1 Discrete Wavelet Transform (DWT)

The different frequency coefficients are obtained from the spatial domain using Low Pass Filter (LPF) and High Pass Filter (HPF) with decimation by 2 as shown in Figure 1 [20].
.
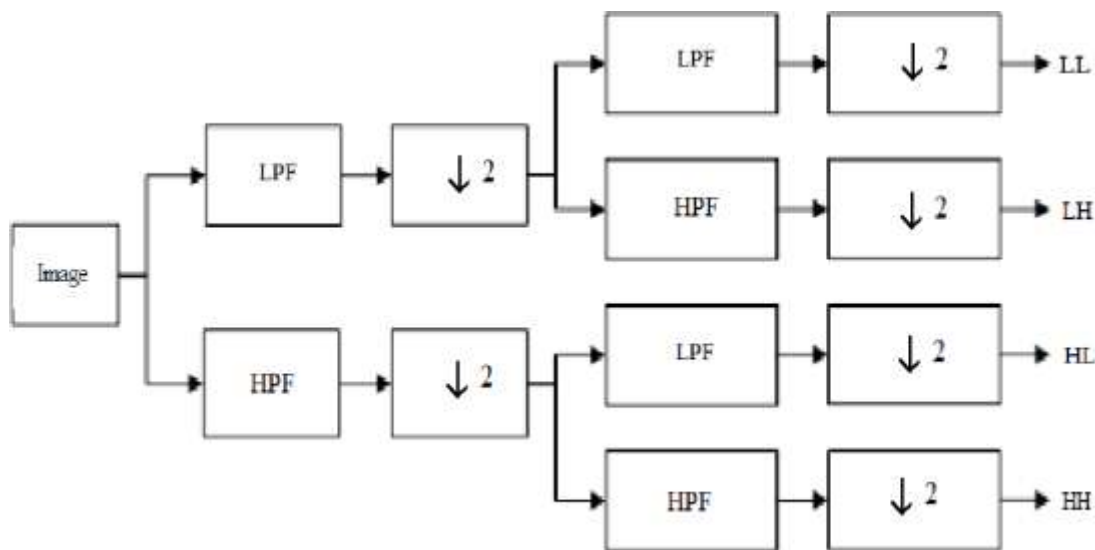
Fig 1. DWT decomposition

The authentic photograph is attached thru LPF and HPF to achieve low and high frequency components. The low frequency component LL subband has crucial facts from the authentic photograph. The LH subband carries negligible facts from the authentic photograph concerning horizontal area information with a high frequency component. The authentic photograph is connected thru HPF and LPF to achieve the high frequency components represented via way of means of the HL subband, which includes negligible facts approximately the authentic photograph concerning longitudinal area information. The high frequency components HH subband received from the authentic photograph is surpassed thru the HPF, and the HPF has negligible facts from the authentic photograph concerning the diagonal area details. The quantities of LL, LH, HL, and HH photograph matrix of length 2X2 are received with the use of equations 1- 4 [21].

$$X = \begin{bmatrix} a & b \\ c & d \end{bmatrix}$$

$$LL = \frac{a+b+c+d}{2}$$

(1)

$$LH = \frac{a+b-c-d}{2}$$

$$(2)$$

$$HL = \frac{a-b+c-d}{2} \tag{3}$$

$$HH = \frac{a-b-c+d}{2} \tag{4}$$

3.2. Canny Edge Detection

It is a process of identifying portions in an image where the illumination of pixel intensities variations for the outcome of the borders of things in an image [22, 23]. The discontinuities in brightness detected permit users to witness the features of an image for important changes in the gray levels. This texture indicates the termination of one region in the image and the start of another. It decreases the quantity of information in an image and conserves the structural possessions of an image. It is used for image segmentation and data extraction in the areas of image processing, computer vision, and machine vision.

some of the most commonly used edge finding methods are Prewitt edge detection, Sobel edge finding, Laplacian edge detection, and Canny edge detection. The most regularly Canny edge finding is used which is an effective and multi-stage algorithm for the detection of a wide range of edges. The drawback of using edge detection is the size of the edge detected output image will be shrunk leading to loss of valuable information, especially from the edges of the input image. The formula for output edge detected image size is (n-r+1)*(n-r+1) if the size of the input image is n*n and the filter size is r*r. For example, if the size of the input image is 6*6 and after applying 3*3 filter, then the output edge detected image is only 4*4. The drawback of edge detection technique is eliminated by padding the input image before applying detection to avoid losing the valuable information in the input images.

3.3. Guided filter:

It is the quickest edge-maintaining filters, because of a neighborhood linear system, which generates the productivity via way of means of seeing the content material of a steering photo, that is the real enter photo itself or an extra diverse photo [24]. The guided clear is an edge-maintaining knocking down operative just like the usual bilateral clear [25]. The guided clear-out has stepped forward results close to edges because bilateral filters, every now and then have undesirable gradient reversal artifacts and motive photo alteration. The guided clear-out has widely wide-spread notion outdoor smoothing and can also relocate the systems of the steering photo to the filtering yield. The guided clear is a quick and non-approximated linear time clear out, and computational hassle is impartial to the filtering kernel length and the depth array [26-28]. This clear out has endless ability in laptop imaginative and prescient and graphics, with its simplicity, efficiency, excellent visible quality, excessive speed, and simplicity of implementation, the guided clear out has witnessed diverse packages in actual products, inclusive of photo modifying apps.

4. Projected Technique:

This section explains the projected SR system using blend of DWT subbands and filtering. The Block diagram of the projected method is shown in Figure 1.
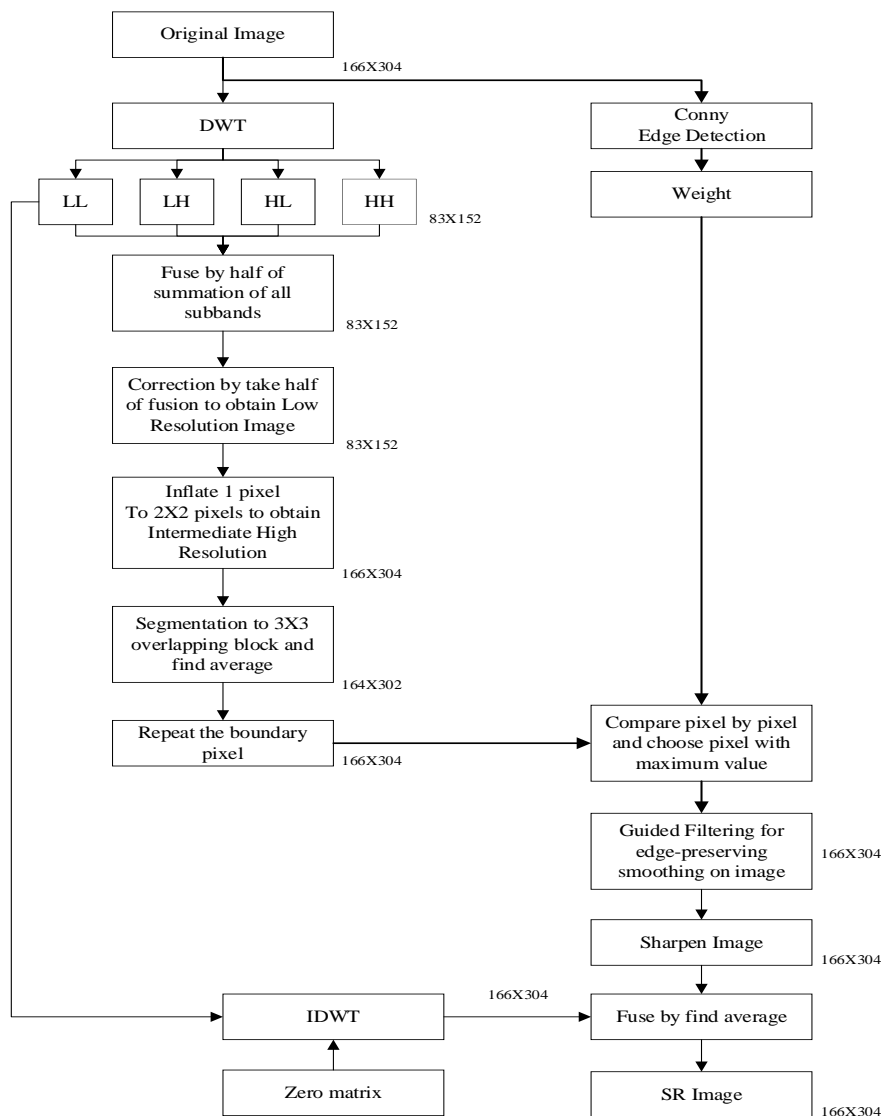
Fig. 1 The Block diagram of the proposed model

4.1 LR images using DWT

The colour images of different sizes are converted into greyscale images with a uniform size of 166X304 to increase computation speed and decrease hardware complications in real-time systems. The procedure of downsampling is applied using DWT on the original image to obtain four sub-bands LL, LH, HL, and HH as shown in Figure 2. The 4 subbands of DWT are fused by summations and divided by two to obtain Low Resolution (LR) images of size 83X152 as shown in Figure 3.

(a) Original Image

(b)LL Image   (c) LH Image

(d)HL Image   (e) HH Image
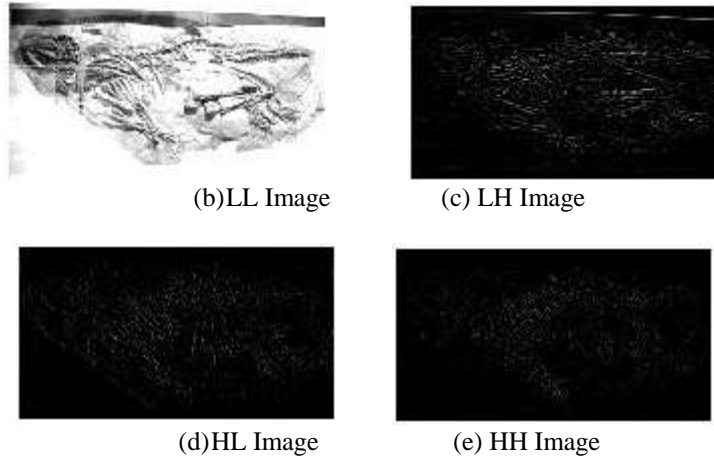
Fig. 2 DWT on original image

Fig. 3 Low-Resolution Image (83x152)

4.2. HR images using inflate and segmentation

The LR images are transformed into intermediate High Resolution (HR) images by expanding each pixel to 4 pixels in the form of 2X2 blocks. The illustration of expansion from 1 pixel to 4 pixels is shown in Figure 4. The 4x4 pixels of LR images are considered to convert into HR images with 8x8 pixels. The single pixel with the value of 32 in the LR image is converted into 4 pixels with the same values of 32 by repeating in the HR image matrics as shown in figure 4(b). The HR image corresponds to the expansion of one pixel into four pixels is as shown in Figure 4 (c).

32	31	35	45
39	44	50	52
31	38	48	55
32	17	7	14

(a) Sample of first 4x4 pixel of Low-Resolution Image

32	32	31	31	35	35	45	45
32	32	31	31	35	35	45	45
39	39	44	44	50	50	52	52
39	39	44	44	50	50	52	52
31	31	38	38	48	48	55	55
31	31	38	38	48	48	55	55
32	32	17	17	7	7	14	14
32	32	17	17	7	7	14	14

(b) Expand from 1 pixel to 4 pixels

(b)Intermediate High-Resolution Image (166x304)

Fig. 4 The illustration of expansion from 1 pixel to 4 pixels to obtain an HR image

The HR image is segregated into 3X3 overlapping chunks to find the average values of 9 pixels in each segmented block to make the smooth image with the nearest pixel. The average value of the first 3x3 pixels is equal to 34.67, similarly second overlapped average value of 3x3 pixels is equal to 35 and soon. The HR image size is decreased to 164X302 because of averaging as shown in Figure 5. Repeat boundary coefficient to obtain an effective HR image with a size of 166X304 as shown in Figure 6.

32	32	31	31	35
32	32	31	31	35
39	39	44	44	50
39	39	44	44	50
31	31	38	38	48

(a) Sample of first 5X5 pixel of Intermediate High-Resolution Image

32	32	31
32	32	31
39	39	44

$\Rightarrow$ 34.67

(b) Average of 1st 3X3 block

32	31	31
32	31	31
39	44	44

$\Rightarrow$ 35.00

(c) Average of 2nd 3X3 block

31	31	35
31	31	35
44	44	50

$\Rightarrow$ 36.89

(d) Average of 3rd 3X3 block

32	32	31
39	39	44
39	39	44

⇨   37.67

(e) Average of 4th 3X3 block

32	31	31
39	44	44
39	44	44

⇨   38.67

(f) Average of 5th 3X3 block

31	31	35
44	44	50
44	44	50

⇨   41.44

(g) Average of 6th 3X3 block

39	39	44
39	39	44
31	31	38

⇨   38.22

(h) Average of 7th 3X3 block

39	44	44
39	44	44
31	38	38

⇨   40.11

(i) Average of 8th 3X3 block

44	44	50
44	44	50
38	38	48

⇨   44.44

(j) Average of 9th 3X3 block

34.67	35.00	36.89
37.67	38.67	41.44
38.22	40.11	44.44

(k) The average pixel matrix of fig (a)

(l) The average pixel image with the size of 164X302

Fig. 5 The average pixel image

34.66667	34.66667	35	36.88889		199.6667	198.6667	198.3333	198.3333
34.66667	34.66667	35	36.88889		199.6667	198.6667	198.3333	198.3333
37.66667	37.66667	38.66667	41.44444	…	199.4444	198.8889	198.7778	198.7778
38.22222	38.22222	40.11111	44.44444		199.2222	199.1111	199.2222	199.2222
35.77778	35.77778	37.88889	42.88889		200.2222	200.6667	201	201
		. . .					. . .	
112	112	112.6667	114		157.2222	156.5556	156.1111	156.1111
110.5556	110.5556	111.1111	112.3333		156.1111	155.1111	154.5556	154.5556
109.4444	109.4444	109.8889	111	…	154.8889	153.8889	153.4444	153.4444
108.3333	108.3333	108.6667	109.6667		153.6667	152.6667	152.3333	152.3333
108.3333	108.3333	108.6667	109.6667		153.6667	152.6667	152.3333	152.3333

(a) repeat boundary coefficients of the average pixel image

(b) The average pixel image after repeating boundary coefficients

Fig. 6 The effective HR image (166X304)

4.3. Edge detection

The edge detection using a canny filter is used to spot the edges of the original image as shown in Figure 7. The weights for the edge detection image vary between 0 to 255 and the weight of 27 is selected to use in this work.
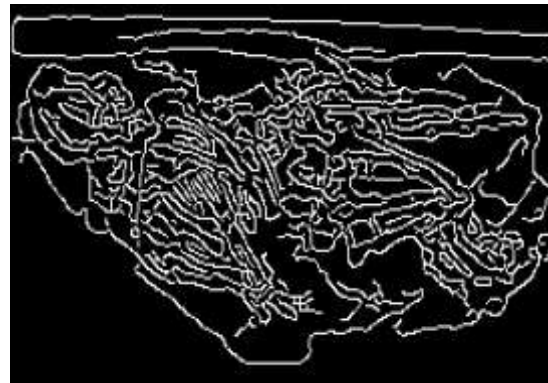
(a) Original Image   (b) Conny edge detected image

Fig. 7 Edge detection

4.4. Pixel values comparison between HR image and Canny edge detected image

The HR image and canny edge detected image are compared pixel by pixel then, choose the maximum pixel values between the two images to enhance the information at the edge of the image is shown in Figure 8.

Fig. 8 The image with maximum pixel values between HR and edge detection images

4.5. Guided filter

The quality of an image is enhanced using guided filtering by edge-preserving, smoothing on an image, and edge sharpening is applied to the image with maximum pixel values between HR and edge detection image to obtain better HR image as shown in Figure 9.

Fig. 9 The sharper HR image

4.6. Super Resolution (SR) Image

The LL sub-band matrix of size 83x152 of the initial original image is considered and zeros are padded to convert LL sub-band matrix into 166x304 size . The IDWT is used on LL sub-band matrix to get an image of size 166x304 as shown in Figure 10.

Fig 10. IDWT image (166x304)

The sharper HR image is fused with the IDWT image by finding the average values to attain the SR Image as shown in Figure 11.

Fig. 11 Super Resolution image

5 Projected Algorithm:

Problem Definition: The new concept of image SR using DWT, expand quantities, edge detection and segmentation to improve the quality of the SR image is introduced.

Objectives: The projected system is established to rise resolution in images for a diversity of applications with the following drives:

(i)   To decrease image noise
(ii) To rise in PSNR and SSIM values

The algorithm of the expected technique verified with a huge number of various images to improve the quality of SR images is as follows:

Input: LR Images
Output: SR Images

1. The variety of images with dissimilar sizes are taken and converted to a size of 166x304.
2. The DWT is applied on images to get four bands with each band size is of 83x152
3. The four bands are merged by the adding equivalent quantities and the results of coefficients are divided by two to attain an LR image size of 83x152.
4. The intermediate HR images of size 166x304 are obtained from LR images by expanding one coefficient into four coefficients by repeating coefficients.
5. The intermediate HR image is devided into 3X3 overlapping blocks and find the average values of 9 pixels in each block to make a smooth image with a size of 164x302.
6. The decreased smooth image size is increased to 166X304 by repeating boundary coefficients.
7. The edge detection using a canny filter is used to detect the edge of the original image.
8. The Smooth HR image and canny edge detected images are compared and considered maximum pixel values to enhance the information at the edge of the HR image.
9. The guided filtering is used on maximum pixel values HR image for sharpening HR image.
10. The LL sub-band of the original image is considered and padded zeros to get an image size of 166x304.
11. The sharpened image is fused with the IDWT image by finding the average pixel values to obtain the SR Image.

6. Performance Analysis:

The definitions of measuring metrics, investigational outcomes, and comparison results with current approaches are deliberated in this sector.

(i)   Definitions: -
  PSNR: The maximum signal power to the signal noise power ratio. The measured illustration is given in equation 5.

$$PSNR = 20 \log_{10}\left(\frac{MAX_f}{\sqrt{MSE}}\right)$$

(5)

Where
MSE is Mean Squared Error
MAX_f is the maximum intensity value =255

(ii) SSIM: The measurement of image superiority and the resemblance among two images based on brightness, contrast, and structure. It is a image local means, standard deviations, and cross-covariance. The values vary from 0 to 1 and the higher value is the better superiority of an image [29]. It is added reliability with human's image dominance related to the PSNR events

6.1 Investigational Results:

The Images of buildings, and fossils, are used to test the projected model are shown in Figure 12.
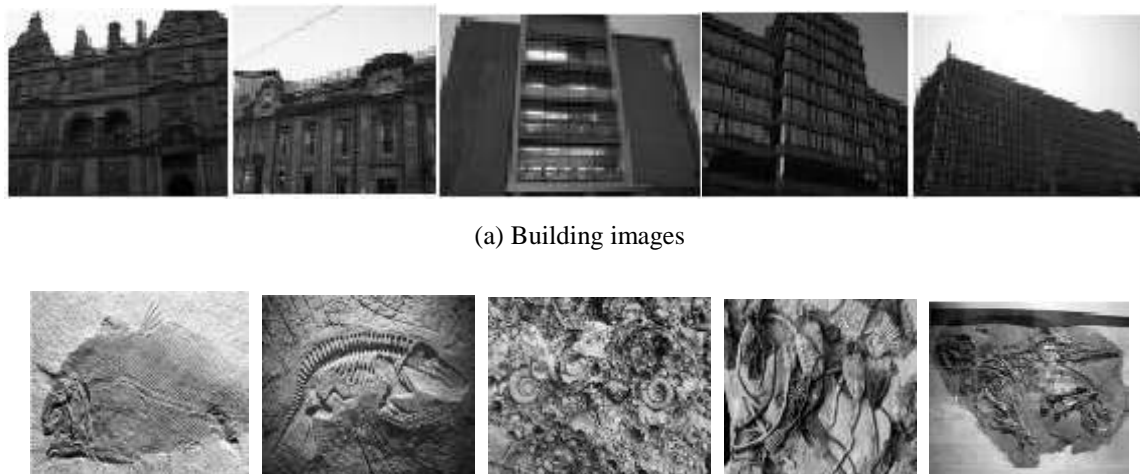
(a) Building images

Fig. 12 Reference Images

The values of performance metricst are based on the kinds of images. The performance of the projected method is verified using the building and fossil images. The values of PSNR and SSIM for different types of building images are given in Table 1 and fossil images are given in Table 2 for LR, and SR images. The SR image values of PSNR and SSIM are high compared to LR images. It is detected that the PSNR and SSIM values are more in the case of building images related to fossil images as the building images are properly observable.

Table1: Performance metrics with Building Images

Sl. No.	LR Images	SR Images	PSNR	SSIM
1			29.0618	0.8968
2			28.8124	0.8995
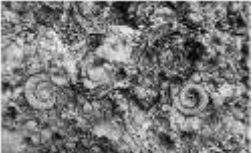
			PSNR	SSIM
3			28.0004	0.9082
4			29.0007	0.8558
5			29.6297	0.8541

Table2: Performance parameters with Fossil Images

Sl. No.	Reference Images	SR Images	PSNR	SSIM
1			26.1219	0.8509
2			25.4785	0.8292
3			22.9387	0.8075
4			35.3285	0.9605
5			25.7122	0.8760

6.2 Projected technique comparison with present methods:

The performance parameters of projected method are compared with existing methods using building and Fossil images presented by Prathibha Kiran, and Fathima Jabeen [30, 31]. It is seen that the PSNR and SSIM values are better in the case of planned technique compared with existing techniques as shown in tables 3 and 4.

Table 3. Comparison of results of the proposed method with current methods using building images

Sl No.	Reference Images	Prathibha Kiran, and Fathima Jabeen [30]		Prathibha Kiran, and Fathima Jabeen [31]		Proposed Method	
		PSNR	SSIM	PSNR	SSIM	PSNR	SSIM
1		25.4298	0.7508	26.8608	0.8134	29.0618	0.8968
2		25.0926	0.7686	26.1693	0.8206	28.8124	0.8995
3		25.0017	0.8257	25.7777	0.8610	28.0004	0.9082
4		26.9860	0.7640	27.8214	0.8184	29.0007	0.8558
5		27.2065	0.7570	28.0269	0.7851	29.6297	0.8541

Table 4. Comparison of results of the proposed method with current methods using Fossil images

Sl No.	Reference Images	Prathibha Kiran, and Fathima Jabeen [30]		Prathibha Kiran, and Fathima Jabeen [31]		Proposed Method	
		PSNR	SSIM	PSNR	SSIM	PSNR	SSIM
1		22.6163	0.6617	23.9256	0.7586	26.1219	0.8509
2		22.5122	0.6499	23.4922	0.7368	25.4785	0.8292
3		20.8675	0.6664	21.6291	0.7462	22.9387	0.8075
4		30.8150	0.8970	34.1496	0.9491	35.3285	0.9605
5		22.6998	0.7380	23.4349	0.7985	25.7122	0.8760

The projected model is also compared with the existing models using Leena and Mandrill images with the performance metrics PSNR as given in Tables 5 and 6. The PSNR values of projected process is related with the existing methods offered by Chunli et al., [32] and Y. Gong et al., [33] using Leena image and seen that the results of our technique is improved on evaluations. The PSNR values of projected technique is related with the present approaches offered by Marija Vella and João Mota [34], and Wenzhe Shi et al., [35] using Mandrill image and viewed that the results of our technique is improved on comparison.

Table 5:The PSNR values with Leena and Mandrill images

Sl. No.	Reference Images	SR Images	PSNR (db)
1	Leena	Leena	31.26
2	Mandrill	Mandrill	30.79

Table 6: The result of proposed method comparison with existing methods

Images	Authors	PSNR (db)
Lena	W. Chunli et al., [32]	26.3786
	Y. Gong et al., [33]	29.2142
	Proposed Method	31.26
Mandrill	Marija Vella and João F. C. Mota [34]	22.91
	Wenzhe Shi et al., [35]	23.72
	Proposed Method	30.79

7. Conclusion:

The SR is an imperative session of image processing techniques in computer vision and image processing, which has an extensive range of real-time applications. The research paper proposed DWT-based Image Super Resolution using Segmentation and Edge Detection for better imagining. The colored images and dissimilar image sizes are transformed into greyscale images with a size of 166x304. The DWT is applied to get four bands and combined to acquire an LR image size of 83x152. The HR images are obtained from LR images by filling one constant into four constants. The HR matrix is divided into a 3x3 overlapped matrix and the average value of every 3x3 matrix is calculated and substituted for the whole HR matrix. The Canny edge detection is used on the original image to get the edge-detected image. The pixel values of HR and canny edge detected images are related and high-value constants are considered. The HR image quality is improved by the guided filter to obtain the improving image. The LL band constants of the original image are expanded by zeros to get a matrix size of 166x304 and IDWT is used to obtain an image. The sharpened image and IDWT images are merged by average value to get the SR image. It is perceived that

the performance of the projected method is enhanced related to present methods. In the future, the GAN technique of deep learning can be used to enhance supplementary outcomes.

References

[1] *W. Li, W. Zhu, and Q. Zhu, "Single-Image Super-Resolution Based on Morphological Component Analysis and Coupled Dictionary Learning In Wavelet Domain," IEEE International Conference on Intelligent Transportation, Big Data & Smart City (ICITBS), pp. 938-941, 2020.*

[2] *F Deeba, S Kun, F Ali Dharejo and Y Zhou, "Wavelet-Based Enhanced Medical Image Super-Resolution," IEEE Access, vol. 8, pp. 37035-37044, 2020.*

[3] *Dinh-Hoan Trinh, Marie Luong, Françoise Dibos, Jean-Marie Rocchisani, Canh-Duong Pham, and Truong Q. Nguyen, "Novel Example-Based Method for Super-Resolution and Denoising of Medical Images," IEEE Transactions on Image Processing, Vol. 23, No. 4, April 2014.*

[4] *Hasan Demirel and Gholamreza Anbarjafari, "Image Resolution Enhancement by using Discrete and Stationary Wavelet Decomposition", IEEE Transactions on Image Processing, Vol. 20, No. 5, pp. 1458-1460, 2011.*

[5] *GungorPolatkan, Mingyuan Zhou, Lawrence Carin, David Blei, and Ingrid Daubechies, "A Bayesian Nonparametric Approach to Image Super-resolution," IEEE Transaction on Pattern Analysis and Machine Intelligence, Vol. 37, No. 2, pp. 346-358, 2015.*

[6] *D. Tran, S. Li-Thiao-Té, M. Luong, T. Le-Tien, F. Dibos, and J. Rocchisani, "Example-based Super-Resolution for Enhancing Spatial Resolution of Medical Images," 38th Annual International Conference of the IEEE Engineering in Medicine and Biology Society (EMBC), pp. 457-460, 2016.*

[7] *J. Chen, X. He, H. Chen, Q. Teng, and L. Qing, "Single Image Super-Resolution based on Deep Learning and Gradient Transformation," IEEE 13th International Conference on Signal Processing (ICSP), pp. 663-667, 2016.*

[8] *Haijun Wang, Xinbo Gao, Kaibing Zhang, and Jie Li, "Single Image Super-Resolution using Gaussian Process Regression with Dictionary-Based Sampling and Student-t Likelihood," IEEE Transactions on Image Processing, Vol..26. No .7. July 2017.*

[9] *Junjun Jiang, Xiang Ma, Chen Chen, Tao Lu, and Zhongyuan Wang, "Single Image Super-Resolution via Locally Regularized Anchored Neighborhood Regression and Nonlocal Means," IEEE Transactions on Multimedia.Vol.19, No 1. January 2017.*

[10] *Oliver Bowen and Christos-Savvas Bouganis, "Real-time Image Super-Resolution using an FPGA, International Conference on Field Programmable Logic and Applications (FPL-2008), pp. 89-94, 2008*

[11] *Weiguo Yang, Bing Xue, and Chunxing Wang, "Image Super Resolution Reconstruction based MCA and PCA Dimension Reduction," Journal Advances in Molecular Imaging, vol 8 no1, pp 1-13, 2018*

[12] *[M. Cao, Z. Liu, X. Huang, and Z. Shen, "Research for Face Image Super-Resolution Reconstruction Based on Wavelet Transform and SRGAN," IEEE 5th Advanced Information Technology, Electronic and Automation Control Conference (IAEAC), pp. 448-451,2021.*

[13] *S Shivagunde and M Biswas, "Single Image Super-Resolution Based on Modified Interpolation Method using MLP and DWT," IEEE International Conference on Trends in Electronics and Informatics, pp. 212-219, 2019.*

[14] *Anand Deshpande and Prashant P Patavardhan, "Survey of Super Resolution Techniques," ICTACT Journal on Image and Video Processing, vol 9, issue 3, pp1927-1934, 2019.*

[15] *Y Zhang, Q Fan, F Bao, Y Liu, and C Zhang, "Single-Image Super-Resolution based on Rational Fractal Interpolation," IEEE Transactions on Image Processing, vol. 27, no. 8, pp. 3782-3797, 2018.*

[16] *Y. Nakahara, T. Yamaguchi, and M. Ikehara, "Single Image Super-Resolution with Limited Number of Filters," IEEE Global Conference on Signal and Information Processing (Global SIP), pp. 36-40, 2018.*

[17] *M. D. Doshi, P. P. Gajjar and A. M. Kothari, "Image Super-Resolution using DWT Based Learning with Zooming Approach," IEEE International Conference on Signal Processing and Integrated Networks (SPIN), pp. 486-491, 2018.*

[18] *C Lien, K Yu and H Chen, "A Novel Image Super-Resolution Technology Based on the Wavelet Coefficients Prediction Scheme," IEEE International Conference on Knowledge Innovation and Invention (ICKII), pp. 13-16, 2018.*

[19] *S. K. Dhara and D. Sen, "Interpolation based on similarity in subband generation for image super resolution," IEEE TENCON, pp. 360-365, 2017.*

[20] *S. Mallat, "A Wavelet Tour of Signal Processing", 2nd ed. San Diego, CA: Academic, 1999.*

[21] *G. V. Sagar, S. Y. Barker, K. B. Raja, K. S. Babu, and Venugopal K R, "Convolution based Face Recognition using DWT and feature vector compression," IEEE International Conference on Image Information Processing (ICIIP), pp. 444-449, 2015*

[22] *J. Canny, "A Computational Approach to Edge Detection," IEEE Transactions on Pattern Analysis and Machine Intelligence, vol. PAMI-8, no. 6, pp. 679-698, November. 1986.*

[23] *P. Bao, Lei Zhang and Xiaolin Wu, "Canny Edge Detection Enhancement by Scale Multiplication," IEEE Transactions on Pattern Analysis and Machine Intelligence, vol. 27, no. 9, pp. 1485-1490, September 2005.*

[24] *K. He, J. Sun and X. Tang, "Guided Image Filtering," IEEE Transactions on Pattern Analysis and Machine Intelligence, vol. 35, no. 6, pp. 1397-1409, June 2013.*

[25] *C. Tomasi and R. Manduchi, "Bilateral Filtering for Gray and Color Images," IEEE International conference on Computer Vision, 1998.*

[26] *S. Li, X. Kang and J. Hu, "Image Fusion With Guided Filtering," IEEE Transactions on Image Processing, vol. 22, no. 7, pp. 2864-2875, July 2013.*

[27] *https://in.mathworks.com/help/images/what-is-guided-image-filtering.html*

[28] *https://in.mathworks.com/help/images/perform-flashno-flash-denoising-with-guided-filter.html*

[29] *Zhou Wang, A. C. Bovik, H. R. Sheikh and E. P. Simoncelli, "Image Quality Assessment: From Error Visibility to Structural Similarity," IEEE Transactions on Image Processing, vol. 13, no. 4, pp. 600-612, April 2004.*

[30] *Prathibha Kiran, and Fathima Jabeen, "Hybrid Domain Feature-Based Image Super-resolution using Fusion of APVT and DWT," Springer Nature International Conference on Recent Advancement in Computer, Communication and Computational Science, Ambient Communications and Computer Systems: RACCCS 2019 (Advances in Intelligent Systems and Computing, 1097) 1st ed. 2020 Edition, pp 401-414, 2019*

[31] *Prathibha Kiran, and Fathima Jabeen, "Wavelet Coefficients Augmentation and Average Segmentation Based Image Super Resolution," International Journal of Application or Innovation in Engineering & Management, vol 10, issue 4, pp 26-39, 2021*

[32] *W. Chunli, L. Cuili, L. Xiaowan and Y. Baoqi, "A New Adaptive Iterative Regularized Algorithm for Super-Resolution Image Reconstruction," IEEE 29th Chinese Control and Decision Conference (CCDC), pp 1315-1322, 2017.*

[33] *Y. Gong, X. Zou, Y. Guo and Z. Dong, "An Experimental Comparison of Super-Resolution Reconstruction for Image Sequences," IEEE 35th Chinese Control Conference (CCC), pp. 5044-5049, 2016.*

[34] *Marija Vella, and João F. C. Mota, "Robust singleimage super-resolution via CNNs and TV-TV minimization," ArXiv: 2004. 00843., 2020.*

[35] *Wenzhe Shi, Jose Caballero, Ferenc Huszár, Johannes Totz, Andrew P. Aitken, Rob Bishop, Daniel Rueckert and Zehan Wang, "Real-Time Single Image and Video Super-Resolution Using an Efficient Sub-Pixel Convolutional Neural Network," IEEE Conference on Computer Vision and Pattern Recognition (CVPR), pp. 1874-1883, 2016*